

INS 57 C 637 C

~~IGEAR 96~~

~~IGC-96~~

1988

IGC -- 96

IGC-96
1988

Thermal Expansion and Phase Transformation Studies on some Materials by High Temperature X-Ray Powder Diffractometry

S. Rajagopalan

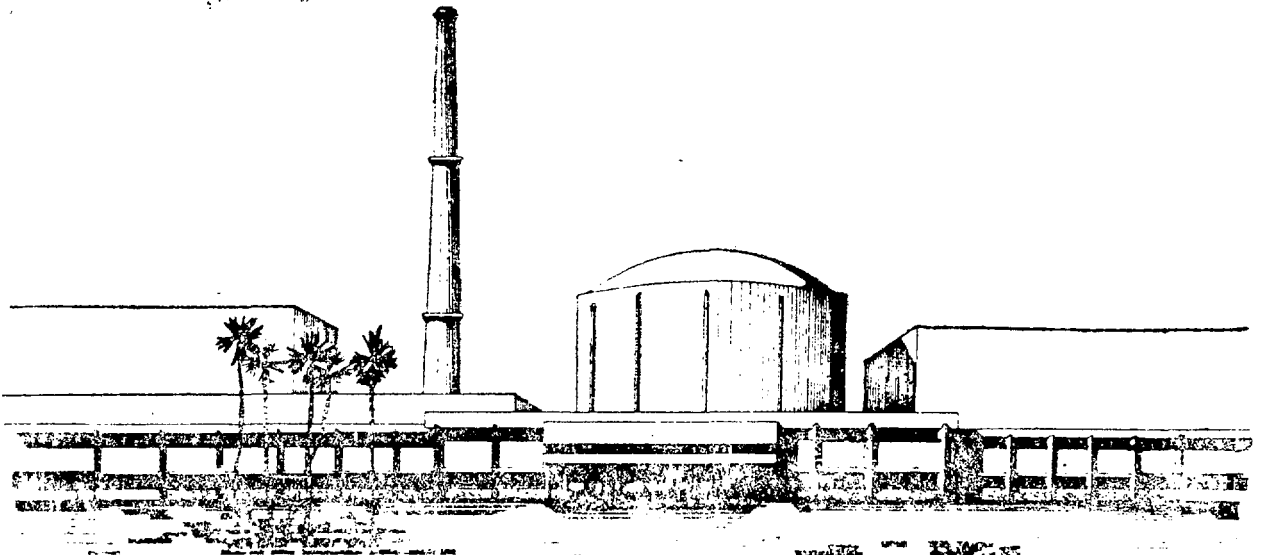
K. V. G. Kutty

H. K. Jajoo

S. K. Ananthkrishnan

R. Asuvatharaman

INDIA
INDIA



GOVERNMENT OF INDIA

DEPARTMENT OF ATOMIC ENERGY

INDIRA GANDHI CENTRE FOR ATOMIC RESEARCH KALPAKKAM

~~IGCAR -- 96~~

~~IGC 96~~
1988

IGC -- 96

GOVERNMENT OF INDIA
DEPARTMENT OF ATOMIC ENERGY

THERMAL EXPANSION AND PHASE TRANSFORMATION STUDIES ON SOME
MATERIALS BY HIGH TEMPERATURE X-RAY POWDER DIFFRACTOMETRY

S. RAJAGOPALAN, K.V.G. KUTTY, H.K. JAJOO,
S.K. ANANTHAKRISHNAN AND R. ASUVATHARAMAN

Indira Gandhi Centre for Atomic Research
Kalpakkam 603 102, Tamil Nadu, India

ABSTRACT

A high temperature chamber based on electrical resistance heating has been integrated to an existing x-ray powder diffractometer. The system is capable of going upto 2500°C at programmed rates of heating. Temperature measurement is carried out by means of Pt/Rh or W/Re thermocouples or by optical pyrometry depending upon the temperature range. Provision exists for performing high temperature x-ray diffractometry in vacuum or in a gaseous atmosphere of low x-ray absorption. The x-ray optical alignment has been ensured by accurately measuring the unit cell lengths of x-ray diffraction standards like silicon and tungsten. The thermocouples have been calibrated within the system by monitoring the melting points of gold and silver. The well characterized transformation of zirconia from the monoclinic to tetragonal structure occurring around 1100°C has been satisfactorily reproduced. The high temperature phase transitions in some rare earth oxides have been studied. Lattice parameter measurements on a variety of materials as a function of temperature upto 1500°C have been carried out and the data found to be in agreement with the literature values. From the measured lattice parameter values, percentage thermal expansion and coefficients of thermal expansion have been calculated for many substances from room temperature to 1500°C.

CONTENTS

	Page
1.0 INTRODUCTION	1
2.0 THE HIGH TEMPERATURE DIFFRACTOMETER CHAMBER	2
2.1 Description	2
2.2 Temperature measurement and control	4
2.3 Operation	5
3.0 EXPERIMENTAL RESULTS	5
3.1 Temperature calibration	6
3.2 System alignment and measurement of accurate lattice parameters	7
3.3 Phase transition	7
3.3.1 Phase transformation of zirconia	8
3.3.2 Phase transformation of rare earth oxides	9
3.3.3 Second order phase transformation	9
3.4 Lattice parameter variation and calculation of percentage thermal expansion	10
3.4.1 Thermal expansion of ceramics, metals and alloys	11
4.0 DISCUSSION	11
ACKNOWLEDGEMENT	14
REFERENCES	15

THERMAL EXPANSION AND PHASE TRANSFORMATION STUDIES ON SOME MATERIALS BY HIGH TEMPERATURE X-RAY POWDER DIFFRACTOMETRY

**S. RAJAGOPALAN, K.V.G. KUTTY, H.K. JAJOO,
S.K. ANANTHAKRISHNAN AND R. ASUVATHARAMAN ***

1.0 INTRODUCTION

X-ray diffraction is one of the methods of characterization of materials in our Laboratory. Study of solid state phase equilibria involving actinide and rare earth materials at high temperatures forms an important part of our work programme. Phase identification at elevated temperatures is usually carried out by quenching the material from the high temperature to the room temperature and subjecting it to x-ray diffraction, assuming the retention of the high temperature phase during the quenching process. However, this procedure may be disadvantageous in certain cases especially when phase changes take place very fast. Hence, it was considered necessary to have a provision for performing simultaneous x-ray diffraction as the sample is heated to high temperature. This would also facilitate the determination of the exact phase transformation temperature. Further, thermal expansion coefficients can be measured by monitoring the change in lattice parameter with temperature.

A diffractometer, rather than a Debye-Scherrer camera, is better adapted for this purpose, for in the former, any angular region of interest can be selectively observed as often as necessary, as and when structural changes are occurring in the material. In the case of camera, prolonged x-ray exposure at any temperature followed by time consuming dark room operations

* The authors are with Radio Chemistry Programme.

should precede the observation of a diffraction pattern, which renders it unfit for recording dynamic phenomena taking place in the material. With this in view, a high temperature chamber (HDK 2, Seifert, West Germany) has been incorporated as an attachment to an existing diffractometer (D 500, Siemens, West Germany) in the Radiochemistry Laboratory, Kalpakkam. The details of the system along with the results of some initial measurements are reported here.

2.0 THE HIGH TEMPERATURE DIFFRACTOMETER CHAMBER

2.1 Description

A cross sectional diagram showing the essential features of the high temperature chamber in position on the diffractometer is given in Fig. 1. The high temperature attachment consists essentially of a cylindrical brass chamber at the centre of which the sample can be mounted. The cylinder of diameter 105 mm and height about 125 mm and of double walled construction is closed at one end and this end is fixed to the vertical goniometer. The body of the chamber is provided with a long beryllium window of thickness 0.5 mm for the incidence and emergence of the x-ray beam in the 2θ angular range 0 to 180° . The other end of the cylinder is provided with a cover carrying four electrodes which extend into the centre of the chamber. Two of these electrodes carry a flat resistor strip of tungsten, molybdenum, tantalum or niobium, which also serve as the sample carrier. The cover flange is held firmly on the cylinder by means of two guide pins to avoid displacement. The sample is thus always held in register with the beryllium window.

In order to minimize heat losses from the sample, the surroundings of the sample are also maintained at a high temperature by means of a U-shaped resistor (shown in Fig.2). This surrounds the sample in such a way as not to block the incident x-rays. This resistor strip is connected to the remaining two electrodes on the flange. Heat shields made of polished foils of tungsten, molybdenum and tantalum are placed between the sample and the flange and also between the sample and the cylinder sides; in the latter shield, there is a cut-out provided towards the beryllium window. The heat shields guard against radiative heat losses. For thermoelectric measurement of temperatures, the thermocouple wires are led through the flange. For temperature measurement by optical pyrometry, two viewing ports fitted with quartz windows are provided on the chamber; either the sample surface or the rear of the sample carrier strip can be viewed, in the latter case through a hole in the surrounding strip.

Through the annular space between the chamber walls, cooling water is circulated when the system is at high temperature. The electrodes are also water-cooled. The heat shields provide protection to the flange. The interior of the chamber has a nickel lining polished to a high gloss so that contamination caused by evaporation and volatilization can be easily removed while cleaning. All connections and feed-through points are vacuum-tight. The chamber is connected to a diffusion pump so that a high vacuum of 10^{-6} torr can be maintained inside; option is available for introducing a protective gas at low pressure through a leak valve.

2.2 Temperature Measurement and Control

The electronic control system consists of the temperature controller, programme generating unit, two thyristor units for regulating the supply of heating current, the thermocouple signal conditioning unit and high current transformers for sample heating (0-10V, 0-100A) and sample environment heating (0-10V, 0-200A). A block diagram of the system organisation is shown in Fig. 3. The high current outputs are fed to the sample carrier and surroundings by brass bayonette connections.

The thermocouple output is used to monitor temperature as well as to control the supply of current to the heating strips so as to keep the sample temperature profile coincident with the programme profile. The desired final temperature as well as the rate of heating/cooling are digitally set at the programme generating unit. The difference between the programme value at any instant and the actual sample temperature at that instant is displayed on a deviation meter on the controller. If the sample temperature falls below the programme value beyond a limit, the programmer is halted till the sample temperature catches up with the programme value. Thus, the sample temperature variation is made to closely follow the programme function. The difference between the final temperature set and the actual temperature at any instant is displayed on a panel meter on the programme generating unit. The current supply for heating is regulated by thyristor firing circuits. The helical potentiometers on the thyristor units are set to pre-determined values, these values being the upper limit of current supplied to the heaters. These current limits should correspond to the desired temperature level and are determined by heating the system in the manual mode where

only the thyristors are involved. The controller compares the temperature of the sample at any instant as measured by the thermocouple with the set final temperature and regulates the supply of current. The current is gradually raised as the sample temperature increases. The incorporation of this control ensures safety of the heaters from excessive currents, should a malfunction develop elsewhere. If the thermocouple circuit breaks by any chance, the controller, and thereby the heating, is automatically switched off.

2.3 Operation

The flange carrying the electrodes is taken off the chamber and clamped on a bracket. The powder specimen is ground to about 50μ in size. It is then placed as a thin layer of thickness about 0.1 mm at the centre of a resistor strip connected stretched to the electrodes. The dimensions of a typical resistor are $50 \times 5 \times 0.1$ mm. A drop of collodion in amyl acetate is used for spreading and binding the sample on the strip. The flange is then replaced on the chamber. After attaining vacuum, heating is commenced at a programmed rate and the temperature measured by means of a millivolt recorder. The diffraction pattern at any temperature is recorded by means of the diffractometer.

3.0 EXPERIMENTAL RESULTS

For most of the measurements, the Pt/Pt-10% Rh thermocouple was used. The junction was made by spot-welding the wires and the junction itself was spot-welded at the back of the specimen carrier strip in order to ensure effective thermal contact.

In order to test the efficiency of the heating chamber and precision in temperature measurement, blank strips were heated several times upto 2000°C at an average rate of 35°/min. The millivolt measurement has been precise to 0.1 mV, thus giving a precision of $\pm 3-4^{\circ}\text{C}$ in the measured temperature.

Some of the x-ray diffractograms were recorded employing Ni-filtered $\text{CuK}\alpha$ radiation in conjunction with a NaI(Tl) scintillation detector with pulse height selection on a strip chart recorder. A secondary beam monochromator of curved graphite crystal was later attached to the diffractometer.

3.1 Temperature Calibration

Temperature measurement is carried out by the Pt/Pt-10% Rh thermocouple upto 1400°C and by the W-3% Re/W-25% Re thermocouple upto 2600°C. Beyond this temperature, optical pyrometry is employed. Following the IPTS recommendations¹, the thermocouples have been calibrated by measuring the melting points of gold and silver inside the system.

A small piece of gold wire was placed on tungsten strip having a dimple at the centre. It was heated at the rate of 35°/min upto 950°C and thereafter at 4°/min., the scintillation detector oscillating about the first two intense peaks of gold all the while. The sharp diffraction lines disappeared abruptly at 1073°C (Fig.4) indicating melting. The heating was arrested at this stage. The pattern here was typical of a liquid. On cooling, the lines reappeared sharply at the same temperature. The same phenomenon was observed at a heating rate of 2°/min from slightly below 1050°C. Repeating the experiment with silver, a

melting point of 980°C was observed and it was not very sharp. A discussion on the limitations of temperature measurement in systems like this may be found in section 4.

3.2. System alignment and measurement of accurate lattice parameters

The basic diffractometer had already been aligned before attaching the high temperature chamber. This was further confirmed with the assembly, by recording a pattern of the x-ray diffraction standard, silicon (NBS, SRM 640a) at room temperature and determining the lattice parameter accurately from the well resolved back reflection peaks using the computer programs due to Taupin² (for indexing and calculation of a) and Werner³ (for refining a). The value obtained for $a = 5.43071 \pm 0.0005\text{Å}$ differs only slightly from the value reported⁴, 5.43088Å . With spectroscopically pure (99.999) tungsten powder (Johnson Matthey) a lattice parameter of $3.1647 \pm 0.0004\text{Å}$ was measured, which compares well with the literature⁴ value of 3.165Å .

3.3 Phase transition

The transformation of a material from one crystallographic phase to another at an elevated temperature can be followed by observing either the disappearance of the sharp lines of the low temperature phase or the appearance of lines of the high temperature phase. Normally phase transitions occur over a range of temperature, the nucleation and growth of crystallites of the new phase controlling the kinetics; some others are abrupt, diffusionless transitions. The particle size and thermal history

of the sample are important in deciding the temperature and rate of the reaction; so also the presence of impurities and water molecules in the sample.

3.3.1 Phase transformation of zirconia

With a view to standardizing a procedure of following high temperature structural changes, we have looked at the well characterized phase transition in zirconia⁴ from the room temperature monoclinic form to the tetragonal form at a temperature range of 800-1200°C. Zirconia powder was ground to 37 μ size and placed on a molybdenum strip. Temperature was measured by Pt/Rh thermocouple. The sample was heated at a rate of 25°/min till about 650°C and 10°/min thereafter. The x-ray detector was kept oscillating at a rate of 2°/min in the 2 θ range of 27° - 37° which encompasses two intense lines each of the two phases. At about 750°C, the monoclinic lines start diminishing and vanish at 1200°C. Heating was arrested at this stage and a full diffraction pattern recorded which was characteristic of the pure tetragonal phase. The system was then cooled at the same rate. At about 850°C, the x-ray pattern indicated coexistence of both the tetragonal and monoclinic phases. Back at room temperature, the pattern corresponded to the pure monoclinic phase, indicating that the transformation is completely reversible. Fig. 5 shows diffraction patterns, before, during and after the transition.

Once the tetragonal phase appears and the heating is arrested, the transformation does not proceed to completion even

after an extended soaking at that temperature. All these observations are in conformity to what is described by Subbarao, Maiti and Srivastava⁵.

3.3.2 Phase transformation of rare earth oxides

From samarium onwards the sesquioxides of rare earths exist in the cubic rare earth C type structure, at room temperature, but transform into the monoclinic rare earth B structure at high temperature. With rising temperature, the materials undergo a series of further transitions and regain the cubic structure before the melting temperature⁶. We have studied the C to B transformation of samaria, europia and gadolinia. The structure changes over a range of temperature. We found the transformations to commence around 900°C for Sm₂O₃, 1100°C for Eu₂O₃ and 1200°C for Gd₂O₃ after soaking for about two hours at the respective temperatures. When the temperatures were elevated further by about 100°C the transformation took place in less than 30 minutes. These results agree with the reported values⁷.

3.3.3 Second order phase transformation

Second order phase transformations can also be followed by high temperatures x-ray diffractometry. At the transition temperatures, the coefficient of thermal expansion of the material exhibits a lambda type anomaly. We have studied the second order phase transformation occurring near the Curie magnetic ordering temperature of nickel. Fig. 6 shows the observed variation of the thermal expansion coefficient with temperature⁸. The measurement of thermal expansion by high temperature XRD is discussed in the next section.

3.4 Lattice parameter variation and calculation of percentage thermal expansion

The unit cell parameters of a crystalline solid change with temperature due to the anharmonic component in lattice vibrations. The lattice parameters also change on solid solution formation. The theoretical density of a material is calculated by measuring the lattice parameter and thereby the unit cell volume. Monitoring the change in lattice parameter as a function of temperature, the thermal expansion coefficients of the material/phase can be calculated. Since the variation involved is very small, a few thousandths of an angstrom, in order to measure it accurately, a high degree of precision must be obtained in the measured lattice parameter values. Precision of the order of a few parts in 10^4 is commonly attained. This method of studying the thermal expansion behaviour is especially attractive in the case of ceramics because the investigation can be carried out with polycrystalline, powder samples. Other methods like dilatometry require specimens compacted to near theoretical density or rods in order to obtain reliable results.

From the measured lattice parameter values the percentage thermal expansion can be calculated using the equation.

$$\text{Percentage thermal expansion at } T = \frac{a_T - a_{298}}{a_{298}} \times 100$$

where a_T denotes the lattice parameter at temperature T and a_{298} that at 298K. The variation of percentage expansion with temperature has been fitted to equations of the form

$$A + B(T - 298) + C(T - 298)^2$$

3.4.1 Thermal expansion of ceramics, metals and alloys

We have studied^{9,10} the variation of thermal expansion and coefficients of thermal expansion of some standard materials like tungsten, alpha alumina and platinum, and of nuclear materials like thoria, samaria, europia and gadolinia and compared the data with literature values¹¹⁻¹⁷. The equations fitted to the variation of percentage expansion of some materials are given below:

$$W: -0.018 + 4.64 \times 10^{-4} (T-298) + 4.05 \times 10^{-8} (T-298)^2$$

$$Al_2O_3: -0.034 + 7.14 \times 10^{-4} (T-298) + 13.19 \times 10^{-8} (T-298)^2$$

$$ThO_2: -0.042 + 8.47 \times 10^{-4} (T-298) + 12.74 \times 10^{-8} (T-298)^2$$

$$Eu_2O_3: -0.044 + 7.57 \times 10^{-4} (T-298) + 8.26 \times 10^{-8} (T-298)^2$$

$$Gd_2O_3: -0.047 + 8.57 \times 10^{-4} (T-298) + 8.37 \times 10^{-8} (T-298)^2$$

Figures 7 - 9 represent the thermal expansion behaviour of some of the above substances.

We have also measured the thermal expansion of the alloy permandur from room temperature to 600°C.¹⁸ Permandur, an alloy of iron and cobalt with traces of vanadium can be used as a magnetostrictive transducer material in liquid sodium technology. Using thin sheets of this substance, its thermal expansion could be measured. Strips resembling the original sample carrier were used and subjected to x-ray diffraction while being heated.

4.0 DISCUSSION

X-ray diffraction measurements at high temperatures are more prone to errors than at room temperature^{19,20}. The errors stem mainly from the geometrical alignment problems at high

temperatures and limitations in temperature measurement. The limitations and errors and how they are mitigated are briefly considered below.

One of the major problems of high temperature diffractometry is sample displacement from the centre of the measuring circle owing to thermal expansion of the sample carrier. Consequently, the focusing condition is offset, which leads to shift in angular positions of reflections. In the present case, this difficulty can be minimized by first raising the temperature slightly higher than the desired value, adjusting the sample carrier strip taut by rotating the relevant electrodes slightly and then coming down to the required temperature.

The presence of the high temperature chamber on the goniometer imposes limitations in the range of 2θ available. But the full 2θ range is not often required to be scanned in the study of high temperature structural changes. In our case, a range from $6-142^\circ$ is attainable.

Thermal gradients across and through the sample cause x-ray line broadening at high temperatures. Since the penetration of a commonly used radiation like $\text{CuK}\alpha$ is less than about 100μ in most metal and ceramic samples, the temperature difference within this depth in the sample will not be more than 2 or 3°C . Temperature gradients are minimised in the present case by heating the surroundings of the sample, and by the presence of the heat shields.

Limitations exist in the measurement of temperature also. Strictly, the thermocouple or any temperature measuring device should monitor the temperature of the sample surface where x-ray diffraction is taking place. This is not always practicable. The

thermocouple can give rise to its own diffraction lines in the angular range of interest, or it can decrease the diffracted intensity from the sample by blocking a part of the irradiated area which is only a few square millimetre. In our case, the thermocouple junction is spot-welded at the rear of the sample carrier where the temperature could differ by only a few degrees from the sample temperature because of the fact that the sample is a thin layer on a metal foil of thickness 0.1 mm.

For temperature measurements by optical pyrometry, the sample should be an ideal black body, a condition difficult to obtain inside the x-ray diffractometer chamber. Emissivity corrections can be applied to the measured temperature if it is ensured that the sample surface is extremely clean, which is possible only in very high vacua. Moreover, there is a heated strip surrounding the sample and this condition makes emissivity corrections inapplicable. However, the presence of the heater strip around the sample slightly improves the conditions of temperature measurement by making the system a rough approximation to a black body. This is evidenced by the fact that the temperatures measured by thermocouples and an optical pyrometer working at 650 nm at the rear of the sample carrier strip differ by only 1% in the region 1100-2000°C. A ratio pyrometer is considered more suitable for temperature measurements in systems of this kind where ideal black body conditions do not exist.

To obviate these limitations in temperature measurement, an internal temperature calibrant like alumina is sometimes mixed with the powder under investigation. The absolute value of the temperature at the specimen surface layer where diffraction

occurs can be obtained by measuring the lattice parameter of crystalline alumina whose thermal expansion as a function of temperature is accurately known. Measurement of lattice parameters of platinum and thoria has also been employed by investigators for absolute temperature determination.

The above factors should be borne in mind while carrying out high temperature x-ray diffractometry. Adequate precaution to minimize errors enables high temperature phase studies involving measurements of lattice parameters, phase transformation temperatures and reflected beam intensities.

ACKNOWLEDGEMENT

We gratefully acknowledge the useful discussions we have had with S/Shri K.C. Srinivas, P. Sriramamurti and B. Saha during the work and the preparation of this report.

REFERENCES

1. F.D. Rossiri, The International Practical Temperature Scale 1968, *J.Chem. Thermodynam* 2 (1970)
2. D. Taupin, *J. Appl. Crystallography* 6 (1973) 380
3. P.E. Werner, *Arkiv fur Kemi* 31 (1969) 513
4. C.R. Hubbard, H.E. Swanson and F.A. Mauer, *J.Appl. Cryst.*8 (1975) 45
5. E.C. Subbarao, H.S. Maiti and K.K. Srivastava, *Physica Status Solidi (A)* 21 (1974) 9
6. *Rare Earths Handbook*, Vol. 3, Ed. K.A. Gschneidner and L.R. Eyring (1979), NHPC, Amsterdam.
7. S. Stecura and W.J. Campbell, *Bur.Mines Rep., Invest. No. 5847* (1961)
8. Mohammed Yousuf, P.Ch. Sahu, H.K. Jajoo, S.Rajagopalan and K. Govinda Rajan, *J.Phys. F: Met.Phys.* 16f (1986) 373
9. H.K. Jajoo, S. Rajagopalan, S.K. Ananthkrishnan, K.V.G. Kutty and C.K. Mathews, Paper presented at the National Symp. on Radiation and Radiochemistry, Bombay, Dec. 1983.
10. S. Rajagopalan, H.K. Jajoo, S.K. Ananthkrishnan, K.V.G. Kutty and C.K. Mathews, Paper presented at the 12th Annual Symp. in Chemistry, IIT Madras, March 1987.
11. R.K. Kirby, *High Temp. High Press.* 4 (1972) 459
12. Y. Waseda, K. Hirata and M. Ohtani *High Temp. High Press* 7 (1975) 221
13. C.R. Houska, *J. Phys. Chem. Solids* 25 (1964) 359
14. *American Institute of Physics Handbook* (1969)
15. M. Hoch and A.C. Momin, *High Temp. High Press* 1 (1969) 401
16. S. Stecura, *Bur. Mines Rep. Invest. No. 6616* (1965)
17. W.J. Campbell, *Bur. Mines Rep. Invest. No. 8107* (1962)
18. IGC-89 (1986), P. 88
19. W.J. Campbell, *High Temperature Diffractometer Techniques;* Chap. 4, *Handbook of X-rays*, Ed. E.F. Kaelble, McGraw-Hill (1967)
20. T. Sakurai and T. Takizaura, *High Temp. High Press* 3 (1971) 325.

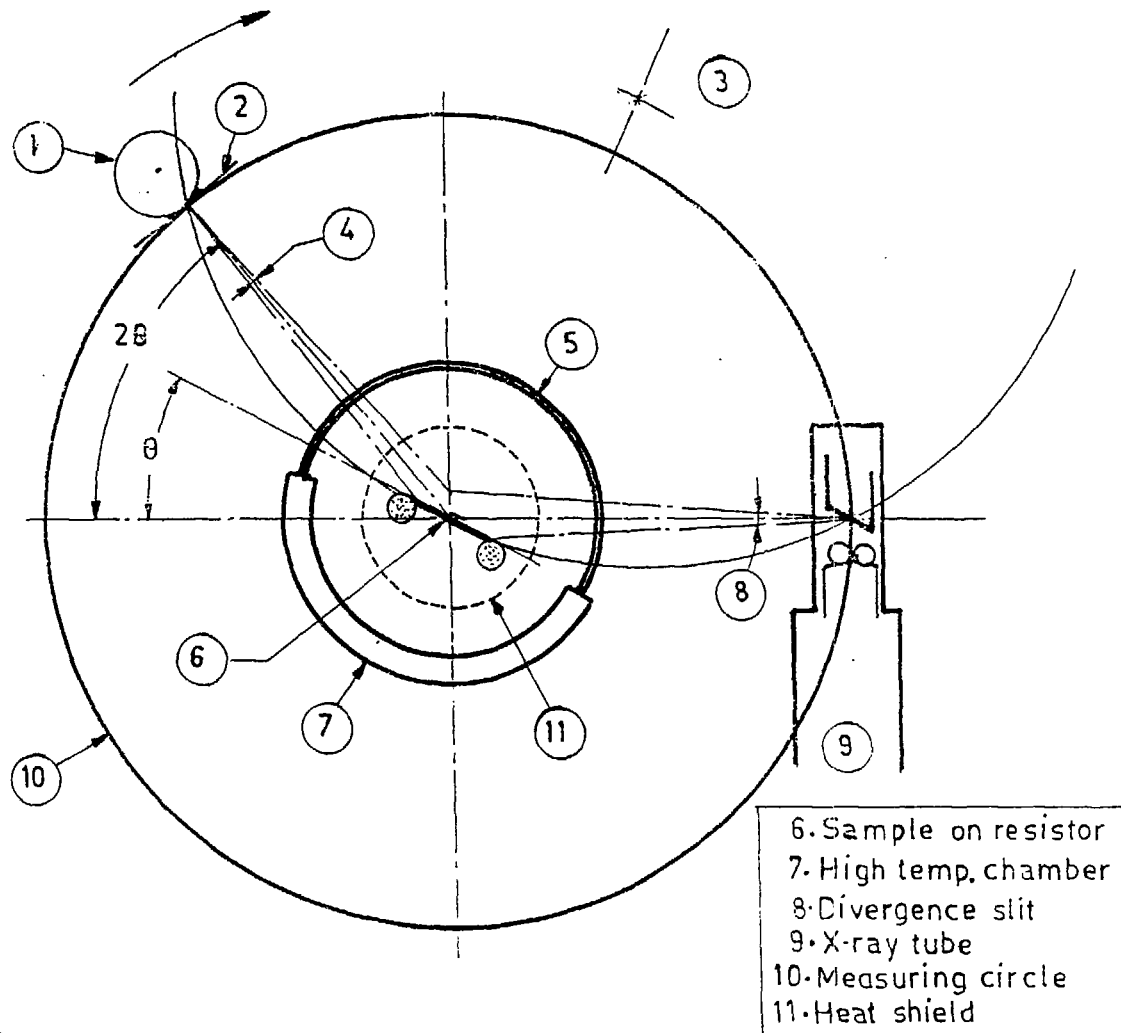


Fig.1 X-ray diffraction geometry incorporating the high temperature attachment.

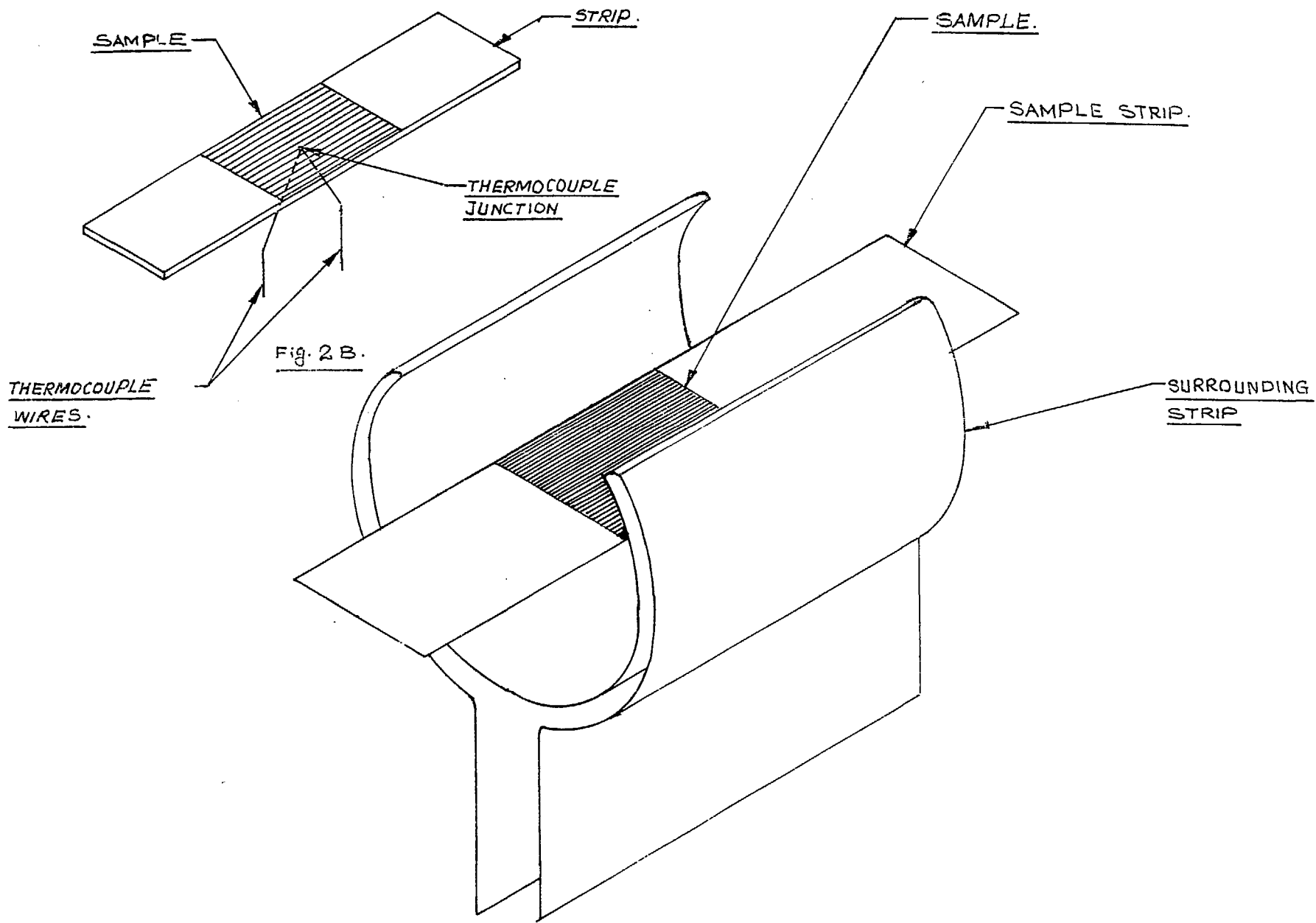


Fig.2 The arrangement of sample strip and surrounding heaters

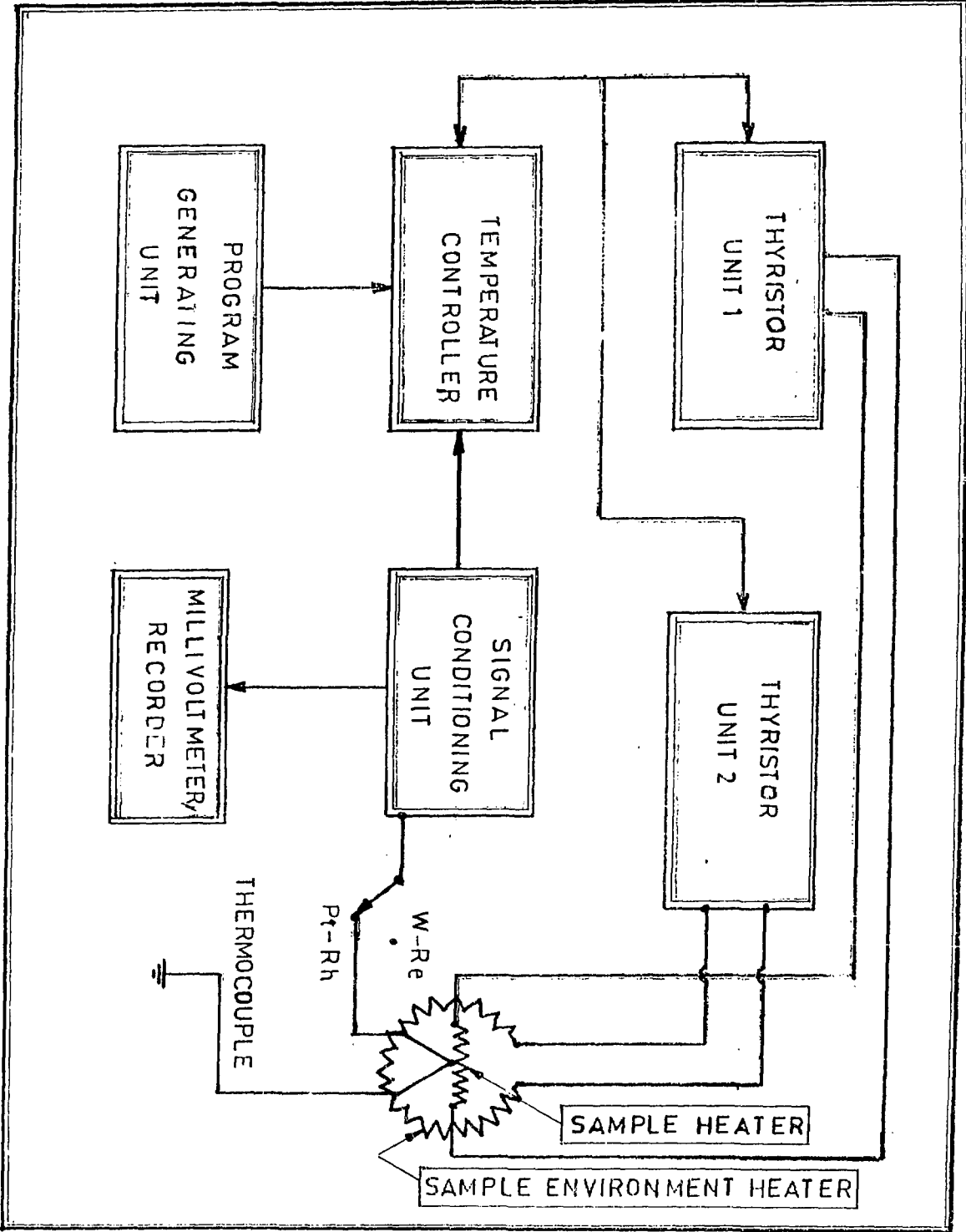


Fig. 3 Schematics of the temperature controller unit

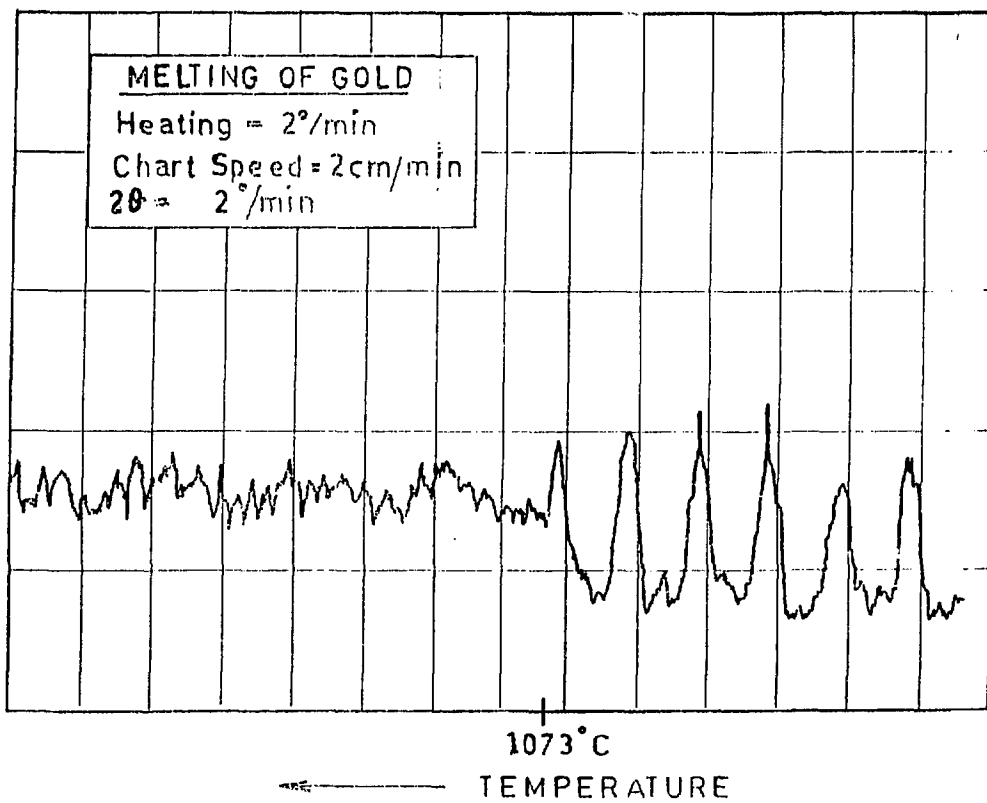


Fig.4 A diffraction peak of gold at the temperature of melting

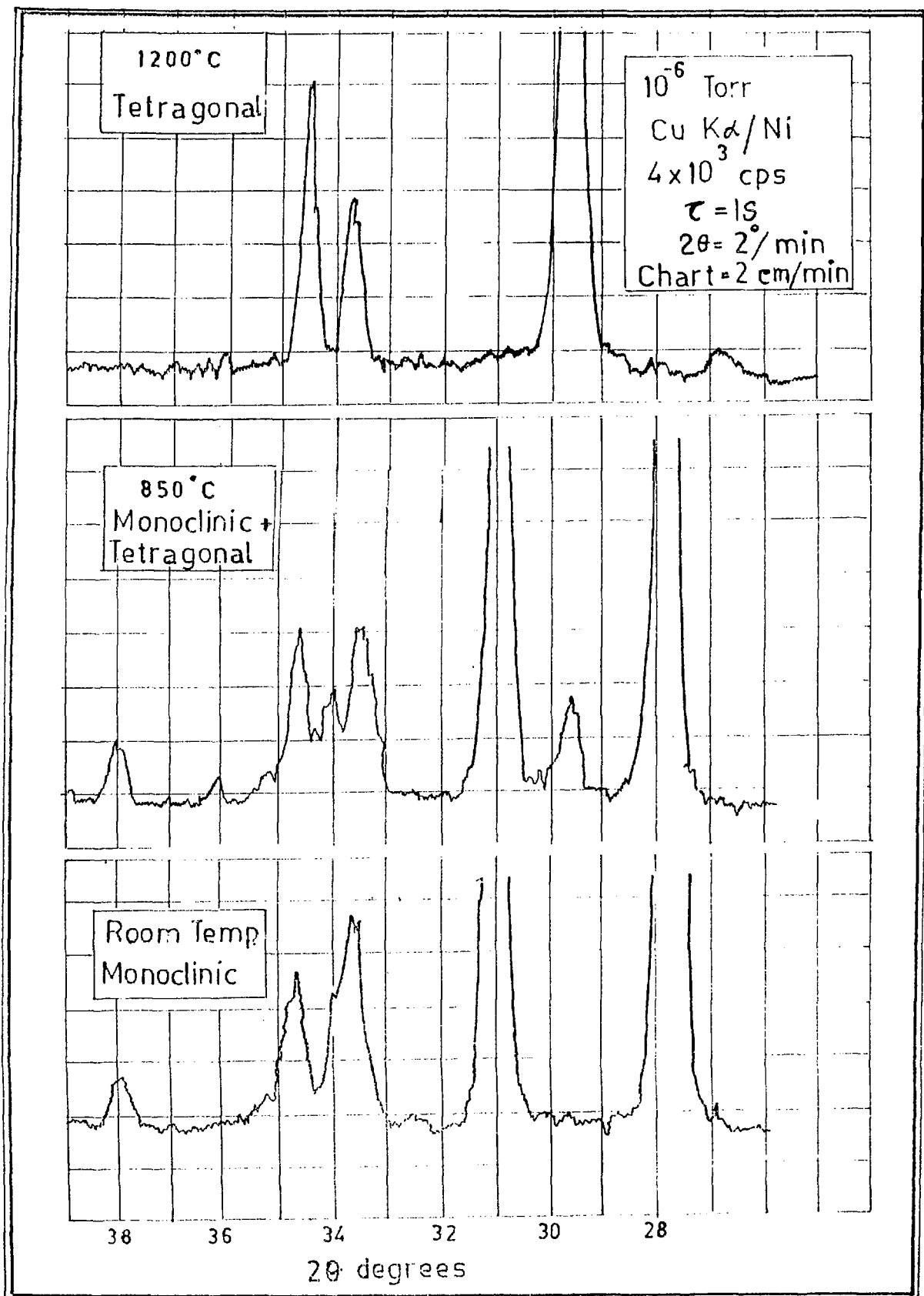


Fig.5 Diffraction pattern of zirconia before, during and after phase transformation

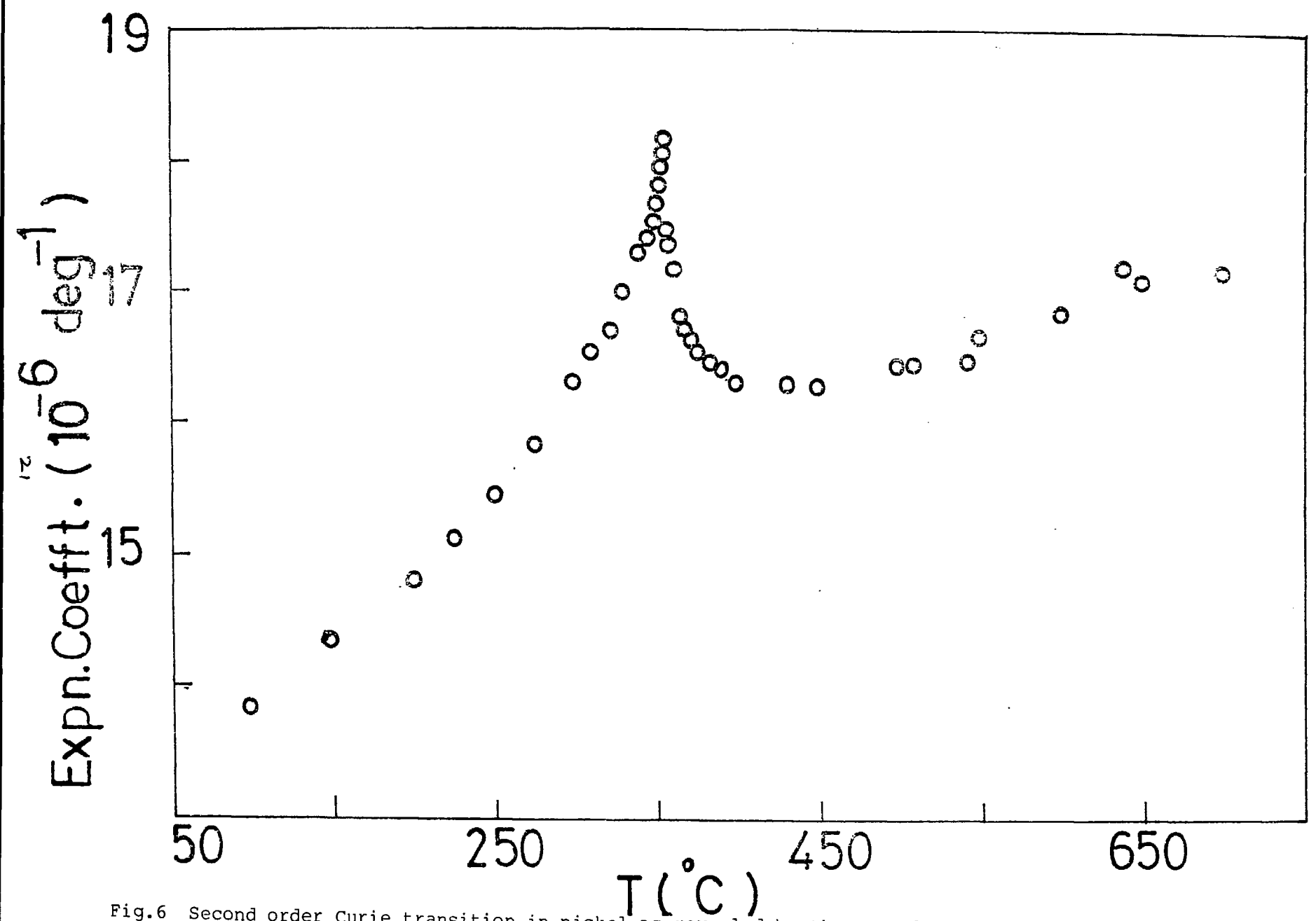


Fig.6 Second order Curie transition in nickel as revealed by the anomalous variation of thermal expansion coefficient with temperature

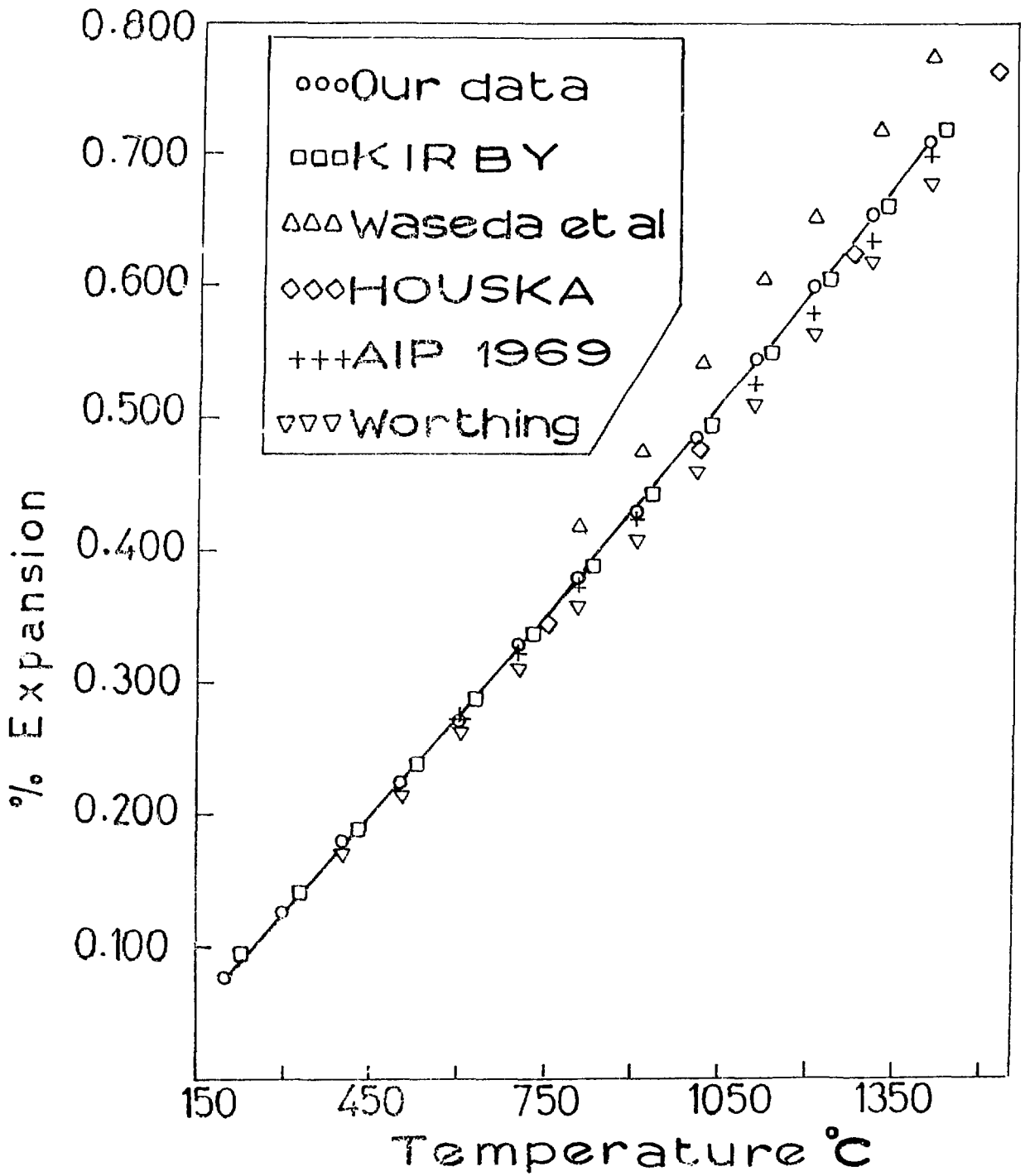


Fig.7 Measured % expansion of tungsten versus temperature as compared with the reported values

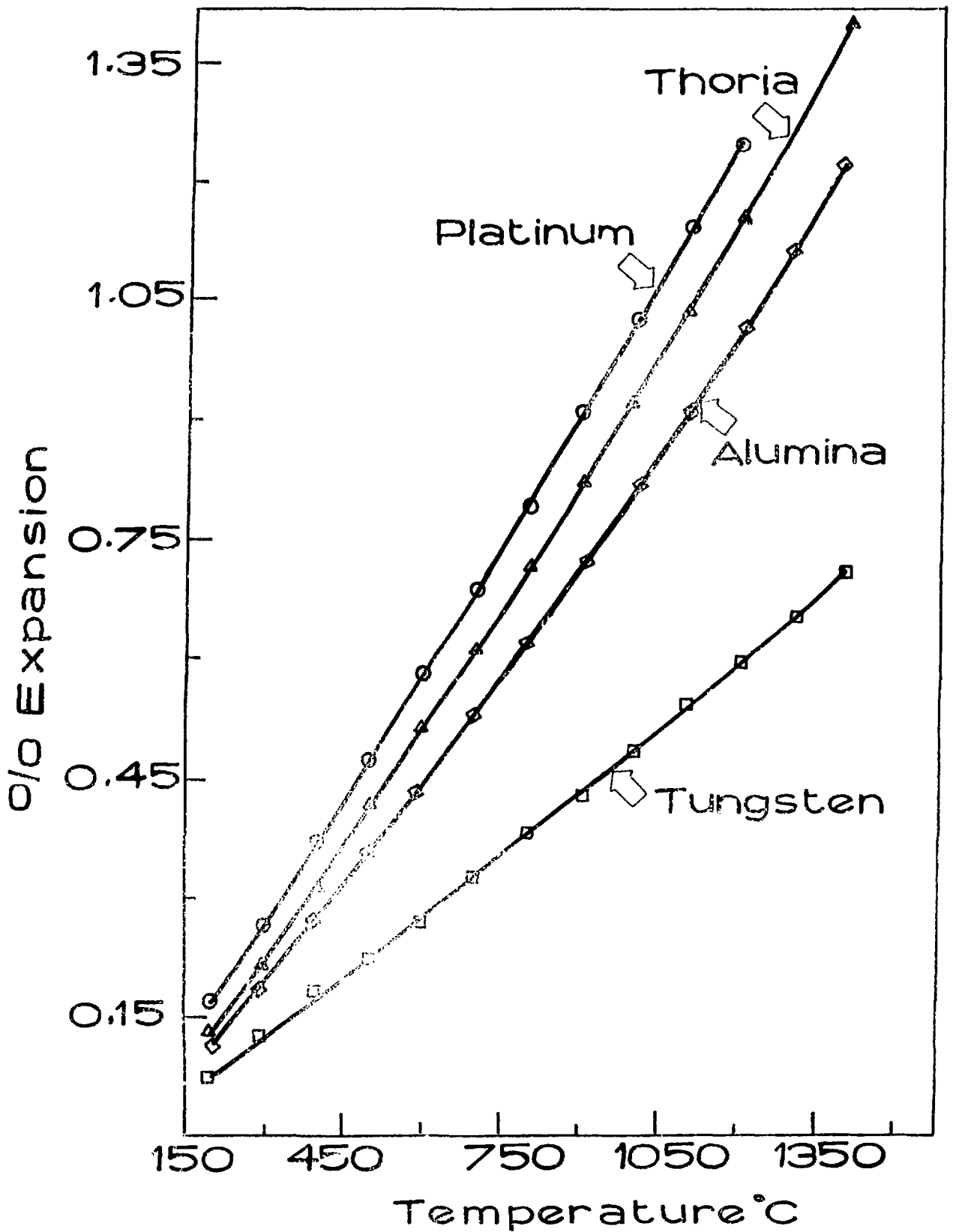


Fig.8 Percentage expansion of the various standards studied as a function of temperature

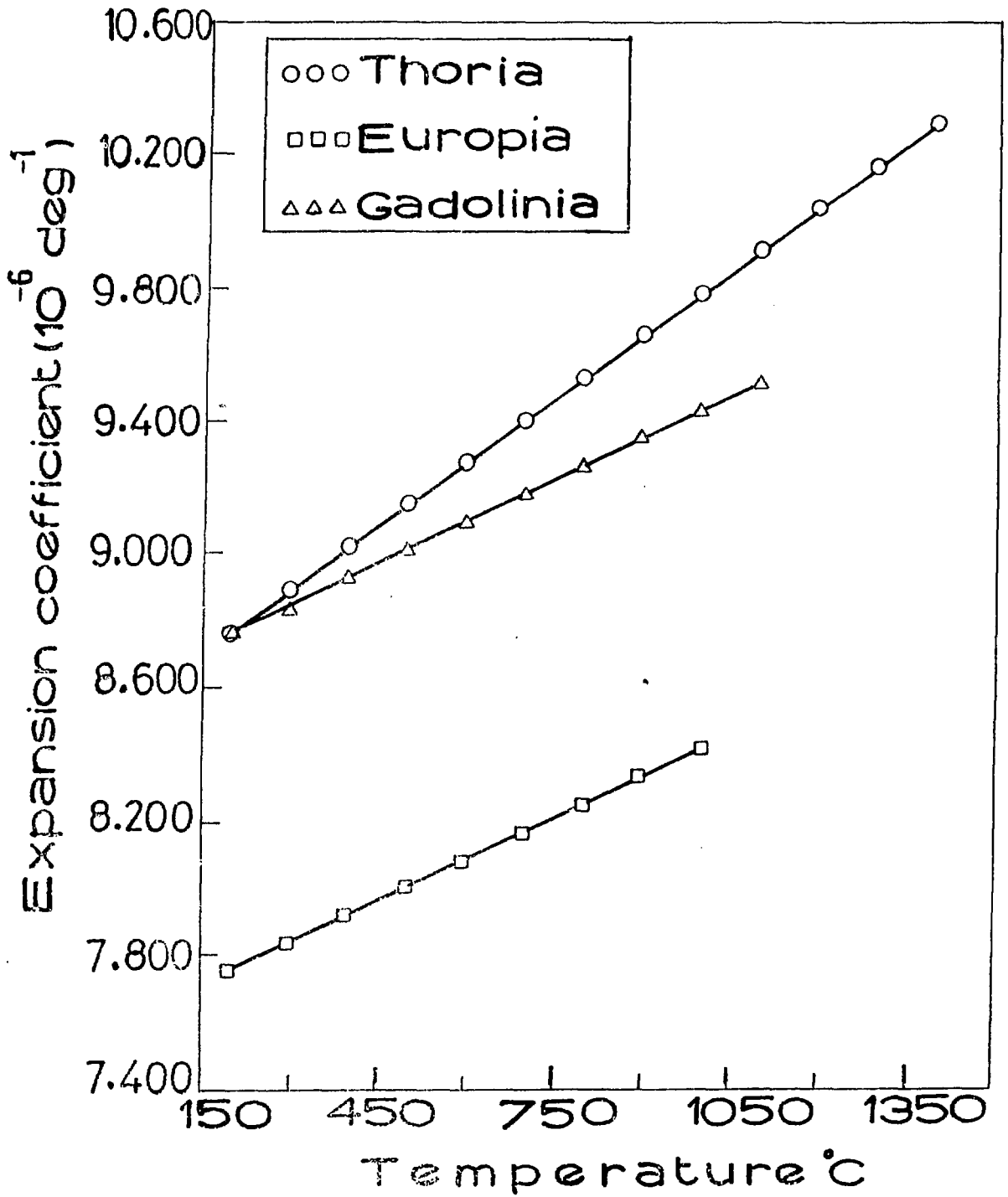


Fig.9 Measured expansion coefficient of thoria, europia, and gadolinia as a function of temperature